# INCORPORATING ANATOMICAL CONNECTIVITY INTO EEG SOURCE ESTIMATION VIA SPARSE APPROXIMATION WITH CORTICAL GRAPH WAVELETS

*David K. Hammond*[1]*, Benoit Scherrer*[2] *and Allen Malony*[1]

[1] NeuroInformatics Center, University of Oregon
[2] Computational Radiology Laboratory, Children's Hospital, Harvard University

*The source estimation problem for EEG consists of estimating cortical activity from measurements of electrical potential on the scalp surface. This is a underconstrained inverse problem as the dimensionality of cortical source currents far exceeds the number of sensors. We develop a novel regularization for this inverse problem which incorporates knowledge of the anatomical connectivity of the brain, measured by diffusion tensor imaging. We construct an overcomplete wavelet frame, termed cortical graph wavelets, by applying the recently developed spectral graph wavelet transform to this anatomical connectivity graph. Our signal model is formed by assuming that the desired cortical currents have a sparse representation in these cortical graph wavelets, which leads to a convex $\ell_1$-regularized least squares problem for the coefficients. On data from a simple motor potential experiment, the proposed method shows improvement over the standard minimum-norm regularization.*

***Index Terms—*** EEG source estimation, sparse representation, inverse problems, graph wavelets

## 1. INTRODUCTION

The goal of functional neuroimaging is to infer information about neural activation within the human brain. However, noninvasive modalities (including fMRI, PET, MEG, and EEG) cannot measure cellular activation directly, and instead make indirect inference based on some other physical measurement process. EEG consists of measuring the time courses of electrical potentials on the surface of the scalp. These potentials are due to current flow through the conductive tissues of the head (volume conduction), arising from dipole current sources reflecting brain activity in the cerebral cortex. Estimating these unknown cerebral source currents from measured potential data is known as EEG source estimation (or source localization), and has important applications for both clinical neurology and basic neuroscience research.

A common approach for this problem is the distributed dipole framework, where the cortical surface is divided into a large number of patches, and current dipoles are placed on each cortical patch. Using an appropriate model for head conductivity, one can determine a linear relationship between the source dipole currents and the measured potentials. The source estimation problem then becomes an underconstrained linear inverse problem as the number of sensors (EEG electrodes) is much smaller than the dimensionality of the cortical sources (typically several thousand). Getting a unique solution requires introducing some form of regularization, e.g. enforcing some prior knowledge about the desired source solution. See [1] for a recent review of different priors used for this problem.

The brain has a highly interconnected structure, with different cortical regions linked to each other by tracts of axonal fibers, which form the brain's white matter. As regions interact with each other by neural action potentials following these fiber connections, it is natural to expect the patterns of anatomical connectivity to influence likely patterns of cortical activity. The development of diffusion weighted MRI imaging has enabled non-invasive measurement of the directionality of white matter. Knowledge of fiber directionality enables tracing fiber streamlines, allowing one to build a detailed, quantitative, subject-specific description of brain connectivity by measuring the number of fiber tract streamlines interconnecting different brain regions.

In this work, we propose a novel methodology for constructing a prior on cortical source activity which uses this connectivity knowledge. We first construct a wavelet frame on the cortical connectome graph, using the recently developed Spectral Graph Wavelet Transform [2], which defines wavelet transforms on arbitrary weighted graphs. These resulting "cortical graph wavelets" have the key property that they are localized in the intrinsic topology of the connectome graph, e.g. their support tends to diffuse out from a central vertex across edges in the graph. This implies that they should be efficient for representing signals that are coherent across graph edges, and localized in the graph. These properties are to be expected of the cortical activation we wish to recover : for many EEG experimental paradigms we are interested in localizing focal brain activity. Additionally, we expect activity to be similar in regions that are strongly connected. These considerations motivate our fundamental signal model - that the desired cortical sources possess a sparse representation in the cortical graph wavelet frame.

We impose this sparsity in an unconstrained optimization formalism by placing an $\ell_1$ penalty on the wavelet coefficients for the cortical sources. When used in conjunction with a quadratic data-fidelity term, this leads to a convex $\ell_1$-regularized least squares problem, which may be solved efficiently by interior point methods. As a preliminary evaluation of our sparse representation with cortical graph wavelets (SR-CGW) method, we compare source estimation of our method and the minimum norm method for data for a simple motor task, showing improved localization, with more focal and easily interpretable results for the proposed method.

## 2. ELECTRICAL HEAD MODELING

The research presented here is done in the context of ongoing work on building accurate numerical models of human head electromagnetics, for EEG and ERP analysis [3]. The EEG electrical potentials result from the effects of current flowing through the head, arising from dipole current sources that are generated as a result of microscopic synaptic currents following neurotransmitter release. In the cerebral cortex, the laminar tissue structure allows these microscopic current sources to align coherently, which may be modeled by macroscopic current dipoles oriented normal to the cortical surface.

The goal of forward electrical head modeling is to calculate the scalp electrical potential arising from any cortical current source. This requires knowledge of both the geometry and conductivity of head tissue. We model the head as purely resistive, with spatially

DH funded by US DoD TATRC Research Grant #W81XWH-09-2-0114

| Scalp | Skull | CSF | GM | WM | Eyeball |
|---|---|---|---|---|---|
| 0.44 | 0.018 | 1.79 | 0.25 | 0.35 | 1.5 |

**Table 1**. Electrical conductivities of head tissues, in $\Omega^{-1}m^{-1}$

varying conductivity given by $\sigma(x, y, z)$. In such a medium, current flux $\vec{J}$ is proportional to the electric field $\vec{E}$, i.e. $\vec{J} = \sigma\vec{E} = \sigma\nabla\varphi$, where $\varphi(x, y, z)$ is the electric potential. Conservation of charge then implies that $\varphi$ satisfies the inhomogenous Poisson equation

$$\nabla \cdot (\sigma\nabla\varphi) = s, \tag{1}$$

with the no-flux boundary condition $\sigma\nabla\varphi \cdot \vec{n} = 0$ on the scalp surface, where $\vec{n}$ is the scalp surface normal vector, and where the scalar function $s$ describes current sources or sinks. We note that this equation is valid in the quasi-static limit, where the current is varying slowly enough so that contributions to the potential from both time-varying magnetic fields and capacitive effects may be ignored. In practice during numerical solution, dipole sources are described by setting $s = 0$ everywhere except at a pair of nearby voxels, where $s$ is set to be positive on one, and negative on the other.

We construct subject-specific models using a high resolution ($1\text{mm}^3$ voxel) T1-weighted MRI image of the head, and performing tissue segmentation to classify each image voxel as one of six tissues (skull, scalp, cerebral-spinal fluid, grey matter, white matter or eyeball). The model conductivity $\sigma(x, y, z)$ is obtained by assigning a constant, isotropic conductivity to each tissue type (see Table 1). We solve (1) using a finite difference method on a regular 3D grid with voxel size 1mm. The solver used implements the alternating direction implicit (ADI) scheme, details may be found in [4].

The distributed dipole formalism relies on solving the forward electrical problem for a fixed set of $N_d$ current dipoles located throughout the grey matter. Once these are fixed we may represent the cortical currents by a vector $J \in \mathbb{R}^{N_d}$, where $J_i$ is denotes the current at the i$^{\text{th}}$ dipole. In this work, we determine the dipole locations by first computing a triangulated mesh of the outer cortical surface, and then partitioning the mesh into 2400 roughly equal-area surface patches (1200/hemisphere). A different cortical surface is computed for each subject, in particular a generic atlas surface is not used. Dipoles are then placed in the center of each patch, and oriented normal to the surface. An example of the partitioning into cortical patches is shown in Figure 1(a).

As equation (1) is linear in $\varphi$, we may use the superposition principle to establish a linear relationship between source currents $J$ and the electrode potentials. Abusing notation, in the following we let $\varphi \in \mathbb{R}^{N_e}$ be the potentials at the $N_e$ electrode locations. These satisfy the linear relationship $\varphi = KJ$, where $K$ is the $N_e \times N_d$ leadfield matrix. Each column of $K$ corresponds to the electrode potentials arising from unit activation of a single dipole, thus $K$ may be computed by repeatedly solving (1) with unit sources placed at the dipoles, and then placing them in the columns of $K$.

All of the tissue segmentation, cortical surface extraction and cortical partitioning is performed using the BrainK software package developed at the NeuroInformatics center, details are in [5].

## 3. CORTICAL CONNECTOME GRAPH CONSTRUCTION

Diffusion Tensor Imaging (DTI) is an MRI imaging modality which enables non-invasive measurements of water diffusion within tissue. The diffusion tensor model describes diffusion as Gaussian; e.g. that flux of water $\vec{F}$ follows Fick's Law $\vec{F} = D\nabla c$, where $D$ is the spatially varying diffusion tensor, and $c$ water concentration. Typically the $3 \times 3$ symmetric diffusion tensor $D$ is estimated at each voxel from a series of diffusion weighted images, which each probe a projection of the diffusion in a specific direction. For a comprehensive overview, see [6]. Our raw diffusion data, taken on a Siemens Allegra MRI, consist of 10 unweighted ($b = 0$), and 60 gradient weighted ($b = 700s/mm^2$) images, all of size $128 \times 128 \times 60$ with 2mm cubic voxels. Diffusion tensors were estimated by least squares fitting using TEEM (`http://teem.sourceforge.net`).

As water present in white matter diffuses preferentially along the direction of the component fiber tracts, DTI can be used to estimate the dominant fiber orientation at each point. By starting at an initial seed point and following the local fiber direction, it is possible to trace virtual fiber streamlines throughout the white matter. Within the past ten years, a large amount of research into tractography algorithms (including many not limited to the diffusion tensor model) has emerged, see [7] for a review.

We construct our cortical connectome graphs by tracing fibers starting from seed points distributed uniformly throughout the white matter, and then counting the number of tracts which connect the cortical patches corresponding to the distributed dipoles. The tractography method we use, developed at the Computational Radiology Laboaratory, differs from simple streamlining through the use of both tensor deflection and directional inertia, which are employed to encourage tract streamlines to pass through regions of reduced anisotropy caused by crossing fibers. Sub-voxel resolution of the tract trajectory is enabled by interpolating tensors through first taking the tensor logarithm, and applying the tensor exponential map after interpolation [8]. At each update step, a new point $p^{k+1} = p^k + v^{k+1}s$ is calculated for fixed step size $s$, where the new tract orientation $v^{k+1}$ is determined by

$$v^{k+1} = \gamma v^k + (1-\gamma)\left(\delta(D^{k+1})^2 v^k + (1-\delta)e^{k+1}\right), \tag{2}$$

where $D^{k+1}$ is the diffusion tensor at point $p^k$, $e^{k+1}$ is the principal eigenvector of $D^{k+1}$, and the parameters $\gamma$ and $\delta$ are the direction inertial momentum and the tensor deflection fraction, respectively. Note in particular that if $\gamma$ and $\delta$ are set to zero, (2) reduces to simple streamlining using the principle eigenvector as tract direction.

The degree of directionality of diffusion at each point is commonly measured by the fractional anisotropy

$$\text{FA} = \sqrt{\frac{(\lambda_1-\lambda_2)^2 + (\lambda_2-\lambda_3)^2 + (\lambda_3-\lambda_1)^2}{2(\lambda_1^2+\lambda_2^2+\lambda_3^2)}} \tag{3}$$

where $\lambda_1, \lambda_2, \lambda_3$ are the eigenvalues of the diffusion tensor. We seed our tractography by placing 30 seed points randomly distributed within each voxel where the FA exceeds 0.4 . Streamlines are terminated by stopping when the fractional anisotropy falls below a specified threshold, or the tract bending angle exceeds a specified threshold. This procedure results in a very large number of tracts, approximately 15 million per subject.

Denote these by $\zeta_k(t)$, for $t \in [0, 1]$, where $k$ indexes the tracts. For constructing the tractography-based connectome, we first remove all but cortico-cortico tracts, defined as those for which the endpoints $\zeta_i(0)$ and $\zeta_i(1)$ are both within 10 mm of the cortical surface mesh. In particular this process removes all cortico-thalamic tracts, which are known to be important for regulating cortical function. We say that the tract $\zeta_k$ connects patches $p_i$ and $p_j$ if either the closest patch to $\zeta_k(0)$ is $p_i$ and the closest patch to $\zeta_k(1)$ is $p_j$, or the converse. This relationship is symmetric as the tractography reveals no information about the direction of the tracts. The tractography-based connectome matrix $A^{tr} \in \mathbb{R}^{N_d \times N_d}$ is given by

$$A^{tr}_{i,j} = \sum_{k\,:\,\zeta_k \text{ connects } p_i \text{ and } p_j} \frac{1}{|\zeta_k|} \tag{4}$$

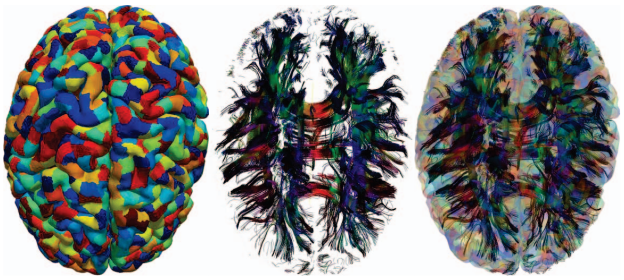

(a) (b) (c)

**Fig. 1**. View of (a) cortical surface mesh (colored to distinguish patches), (b) selected tracts and (c) surface and tracts, superimposed

where $|\zeta_k|$ is the length of tract $k$. Division by tract length is necessary above to compensate for the bias towards longer tracts due to seeding in all regions of white matter.

We have found it useful to include a contribution to the connectome graph derived purely from spatial adjacency of cortical surface patches. This local connectivity graph may be thought of as a very coarse manner of including the effect of local connections between neighboring regions that may not be resolved by the longer-range tractography. We form the local connectivity matrix $A^{loc}$ by setting $A^{loc}_{i,j}$ to be the length of the border (in mm) between patches $p_i$ and $p_j$. This is straightforward to compute given the representation of the patches on the triangular cortical surface mesh; in particular $A^{loc}_{i,j} = 0$ for pair of non-adjacent patches.

We then form the hybrid local/nonlocal adjacency matrix $A = \tau_{tr}A^{tr} + \tau_{loc}A^{loc}$, where the parameters $\tau_{tr}$ and $\tau_{loc}$ control the relative contributions of local vs tractography-cased connectivities. We have fixed $\tau_{loc} = 1 \times 10^{-4}$ and $\tau_{tr} = 5 \times 10^{-1}$ by hand for the results shown here, a more detailed study of the effects of these is an important question for future work.

## 4. SPECTRAL GRAPH WAVELETS

The Spectral Graph Wavelet Transform (SGWT) [2] is a general methodology for constructing wavelet frames for spaces of functions defined on the vertices of finite weighted graphs. Consider a weighted graph with $N$ vertices, and adjacency matrix $A \in \mathbb{R}^{N\times N}$. We may treat any function $f$ on the vertices as a vector $f \in \mathbb{R}^N$. Formally, the SGWT defines the $NK$ wavelets $\psi_{j,n} \in \mathbb{R}^N$, where $1 \leq n \leq N$ indexes the wavelet center vertex, and $1 \leq j \leq K$ indexes the wavelet scale. Crucially, these spectral graph wavelets share many properties of continuous wavelets. They are all zero-mean, localized around their center vertices, and are supported at multiple spatial scales. The SGWT also defines the $N$ scaling functions $\theta_n$, which help to stably represent low-frequency content. In practice, the wavelets $\psi_{j,n}$ and scaling functions $\theta_n$ are not typically explicitly computed, rather the SGWT defines computation of the coefficients $W_f(j,n) = \langle f, \psi_{j,n}\rangle$ and $S_f(n) = \langle f, \theta_n\rangle$ .

The SGWT is defined in the space of eigenvectors of the graph Laplacian operator $L = D - A$, where the diagonal degree matrix $D$ is defined by $D_{i,i} = \sum_k A_{i,k}$. $L$ can be viewed as the graph analogue of the continuous Laplacian operator $-\Delta$. $L$ is symmetric and thus has a complete set of orthonormal eigenvectors $\chi_\ell$ with corresponding eigenvalues $\lambda_0 \leq \lambda_1 \leq ... \leq \lambda_{N-1}$. These $\chi_\ell$ may be viewed as the graph analogue of the complex exponentials $e^{ikx}$ from classical Fourier analysis. They are used to define the graph Fourier transform, where $\hat{f}(\ell) = \langle \chi_l, f\rangle$.

The SGWT coefficients at each spatial scale are given by bandpass filtering $f$, where the filtering is defined in the graph Fourier space. These filters are all given by rescaling, in the graph frequency domain, a single bandpass filter $g$. This wavelet kernel $g$ should behave like a bandpass function, i.e. should satisfy $g(\lambda) \geq 0$ for all $\lambda$, $g(0) = 0$ and $g(\lambda) \to 0$ as $\lambda \to \infty$. The SGWT uses a set of discrete scales $t_j \in \mathbb{R}$ for $1 \leq j \leq K$, both the selection of $g$ and the scales $t_j$ should be viewed as design parameters. The wavelet coefficients at scale $j$ are given by applying the bandpass operator $T_g^{t_j} = g(t_j L)$ to $f$. This operator can be calculated by first observing its action on the eigenvectors, namely $g(t_j L)\chi_\ell = g(t_j\lambda_\ell)\chi_\ell$. By linearity, we see that for $f$ represented in terms of its graph Fourier expansion as $f = \sum_\ell \hat{f}(\ell)\chi_\ell$, we have

$$T_g^{t_j} f = g(t_j L)f = \sum_\ell g(t_j\lambda_l)\hat{f}(\ell)\chi_\ell \tag{5}$$

The wavelets themselves are defined by localizing these operators by applying them to indicator functions on each vertex, e.g. $\psi_{j,n} = T_g^{t_j}\delta_n$, where $\delta_n \in \mathbb{R}^N$ equals 1 on the $n^{\text{th}}$ vertex and 0 elsewhere. The scaling function coefficients and scaling functions are defined analogously as for the wavelets, but with replacing $g$ by a scaling function kernel $h$ which is a lowpass filter (i.e. $h(0) > 0$ and $h(\lambda) \to 0$ as $\lambda \to 0$).

By concatenating all the wavelet and scaling function coefficients of $f$ into a single vector, the SGWT may be viewed as a linear map $W : \mathbb{R}^N \to \mathbb{R}^{(K+1)N}$. This is a $K+1$-fold overcomplete transform. We note finally that naive computation of the coefficients by directly applying (5) would require full diagonalization of $L$, which is prohibitive for large graphs. In practice, the SGWT is computed using a fast transform scheme which relies on Chebychev polynomial approximation of the scaled kernels $g(t_j\lambda)$ over an interval containing the spectrum of $L$, details are in [2].

## 5. SPARSE APPROXIMATION WITH CORTICAL GRAPH WAVELETS

The linear inverse problem we seek to solve is to find current sources $J \in \mathbb{R}^{N_d}$, given electrode potentials $\varphi \in \mathbb{R}^{N_e}$. We cannot simply solve the relation $\varphi = KJ$, as $N_d > N_e$. A common formulation for this is to introduce a prior penalty function $\rho(J)$, and then search for $J$ minimizing the objective function $||\varphi - KJ||_2^2 + \rho(J)$.

We will use a similar regularization framework, but with our objective function and prior defined in the space of wavelet coefficients. $J$ has the cortical graph wavelet expansion $J = \sum_{j=0,n}^{K} c_{j,n}\psi_{j,n}$, where for convenience we set $\psi_{0,n} = \theta_n$. This expansion may be written as $J = W^T c$, where $c \in \mathbb{R}^{(K+1)N_d}$ is a vector of all the coefficients $c_{j,n}$, and $W \in \mathbb{R}^{(K+1)N_d \times N_d}$ is the matrix representation of the entire SGWT.

We impose the desired sparsity by penalizing the $\ell_1$ norm of the coefficients $c$; this is motivated by the extensive literature detailing the connection between wavelet sparsity and $\ell_1$ regularization (e.g. [9]). This leads to the minimization problem

$$c^* = \underset{c}{\operatorname{argmin}}\, ||\varphi - KW^T c||_2^2 + \tau||c||_1, \tag{6}$$

where we have introduced the regularization parameter $\tau$. Once $c^*$ is found, the cortical sources are given by $J^* = W^T c$. For results in this work we take $\tau = 10^{-2}$, as set by hand.

The minimization (6) is an $\ell_1$-regularized least squares problem, also known as the Lasso [10]. The problem is strictly convex, and so admits a unique minimizer. For results in this paper, we solve (6) using the l1_ls software package [11], which employs an interior-point method employing preconditioned conjugate gradients. This algorithm does not require explicit formation of the matrix $KW^T$, and may be used by providing it a function to compute the matrix-vector product. This is significant for our work as we compute the

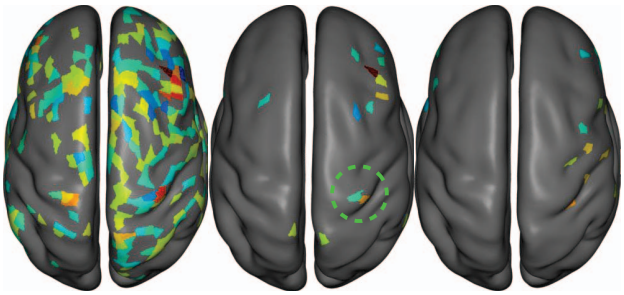

(a) (b) (c)

**Fig. 2**. Comparison of source estimation on ERP data for (a) minimum norm, (b) proposed SR-CGW, (c) sparse dipole method, 40 ms before LT button press, shown on inflated cortical surface. Values below 15% of maximum are thresholded (to grey)

matrix-vector product $W^T c$ using the fast SGWT polynomial approximation scheme.

## 6. RESULTS

As a preliminary indication of the utility of the proposed method, we present source estimation results for data collected from a simple motor task. In this study, collected at the University of Oregon, subjects had high density (256 channel) EEG recorded while performing a button pressing task (left/right thumb/pinky) in response to a visual cue (color change of fixation point). Data for each of the four digits were averaged over a large number ($> 100$) of trials, synchronized by time of button press, to generate the event related potential (ERP)'s.

Under this experimental paradigm, activation is expected in the contralateral hemisphere, localized to the "hand knob" region of motor cortex [12]. Thus the degree to which estimated source activity fits this expectation provides a qualitative evaluation of algorithm performance. In Figure 2 we show source estimates for single subject, for the left thumb condition, 40 ms before the button press. We compare the proposed SR-CGW method against the standard minimum norm solution, and against a third "sparse dipole" method.

The minimum norm solution does show activity in the expected area, indeed with a strong peak (Fig 2a, patch colored red) on the right precentral gyrus, however, the solution is very diffuse. In contrast, the proposed SR-CGW solution (Fig 2b) shows focal activity in the expected area (shown circled in dashed green), and is sparser, with much less extraneous activation. As a simple test to see if this apparent improvement might just be due to general sparsity-promoting effect of our regularization, without really exploiting the anatomical information encoded in the cortical graph wavelets, we examined the sparse dipole method where the $\ell_1$ penalty is applied directly in the dipole domain, rather than in the cortical graph wavelet coefficient domain (Fig 2c). It is computed by solving the optimization

$$J^* = \underset{J}{\operatorname{argmin}} \, ||\varphi - KJ||_2^2 + \tau ||J||_1 \qquad (7)$$

The sparse dipole solution is sparser than the proposed approach, but appears to produce activity in a shifted location, within the central sulcus. This comparison provide evidence that the SR-CGW method is truly exploiting the anatomical connectivity, and at least in some cases improves upon the standard minimum norm solution.

## 7. CONCLUSION

We have introduced a novel regularization framework for the EEG source estimation problem which incorporates anatomical brain connectivity information. This approach relies on estimating a weighted connectivity graph computed from diffusion tensor imaging, where the vertices correspond to the distributed dipoles used in the forward electrical head model. We form the cortical graph wavelet frame by applying the spectral graph wavelet transform construction to this connectivity graph. Our sources are then estimated by assuming they possess a sparse representation in the cortical wavelet frame, leading to an $\ell_1$ regularized least squares problem. The proposed method shows improvement over the standard minimum norm for estimation of ERP sources in a simple motor task.

While the results presented here are promising, both the performance and space of design parameters of the SR-CGW method need to be explored more carefully. The effects of many of the free design parameters of the SGWT used (number of scales $K$, wavelet kernel $g$), as well as parameters related to the graph construction including $\tau_{tr}$ and $\tau_{loc}$ should be more systematically explored. Another important question is whether the method can be modified to make use of knowledge of thalamo-cortical connectivity, which is currently ignored. Finally, as presented the SR-CGW approach operates at each timepoint independently, and so cannot model or exploit temporal correlation in the desired cortical sources. This raises the question of how to formulate joint spatiotemporal estimation with the SR-CGW.

## 8. REFERENCES


[1] R. Grech, T. Cassar, J. Muscat, K. Camilleri, S. Fabri, M. Zervakis, P. Xanthopoulos, V Sakkalis, and B.Vanrumste, "Review on solving the inverse problem in EEG source analysis," *Journal of NeuroEngineering and Rehabilitation*, vol. 5, no. 1, pp. 25, 2008.

[2] D. Hammond, P. Vandergheynst, and R. Gribonval, "Wavelets on graphs via spectral graph theory," *Applied and Computational Harmonic Analysis*, vol. 30, pp. 129 – 150, 2011.

[3] A. Malony, A. Salman, S. Turovets, D. Tucker, V. Volkov, K. Li, J. Song, S. Biersdorff, C. Davey, C. Hoge, and D. Hammond, "Computational modeling of human head electromagnetics for source localization of milliscale brain dynamics," *Medicine Meets Virtual Reality*, 2011.

[4] A. Salman, S. Turovets, A. Malony, J. Eriksen, and D. Tucker, "Computational modeling of human head conductivity," in *International Conference on Computational Science*. 2005.

[5] K. Li, *Neuroanatomical Segmentation in MRI Exploiting A Priori Knowledge*, Ph.D. thesis, University of Oregon, Department of Computer and Information Science, 2007.

[6] S. Mori, *Introduction to Diffusion Tensor Imaging*, Elsevier, 2007.

[7] Y. Assaf and O. Pasternark, "Diffusion tensor imaging (DTI)-based white matter mapping in brain research: A review," *Journal of Molecular Neuroscience*, vol. 34, pp. 51–61, 2008.

[8] V. Arsigny, P. Fillard, X. Pennec, and N. Ayache, "Log-euclidean metrics for fast and simple calculus on diffusion tensors," *Magnetic Resonance in Medicine*, vol. 56, no. 2, pp. 411–421, 2006.

[9] D. Donoho and M. Elad, "Optimally sparse representation in general (nonorthogonal) dictionaries via l1 minimization," *Proceedings of the National Academy of Sciences*, vol. 100, no. 5, pp. 2197–2202, 2003.

[10] R. Tibshirani, "Regression shrinkage and selection via the lasso," *Journal of the Royal Statistical Society. Series B (Methodological)*, vol. 58, no. 1, pp. pp. 267–288, 1996.

[11] Seung-Jean Kim, K. Koh, M. Lustig, S. Boyd, and D. Gorinevsky, "An interior-point method for large-scale l1-regularized least squares," *Selected Topics in Signal Processing, IEEE Journal of*, vol. 1, no. 4, pp. 606 –617, dec. 2007.

[12] T A Yousry, U D Schmid, H Alkadhi, D Schmidt, A Peraud, A Buettner, and P Winkler, "Localization of the motor hand area to a knob on the precentral gyrus. A new landmark.," *Brain*, vol. 120, no. 1, pp. 141–157, 1997.